

Supplementary Information for

Accelerated Charge Transfer in Water-Layered Peptide Assemblies

Kai Tao, Joseph O' Donnell, Hui Yuan, Ehtsham. U. Haq, Sarah Guerin, Linda J. W. Shimon,
Bin Xue, Christophe Silien, Yi Cao, Damien Thompson, Rusen Yang, Syed A. M. Tofail, Ehud
Gazit

This PDF file includes:

Materials and Methods
Figs. S1 to S9

Other Supplementary Materials for this manuscript include the following:

Cif files S1 to S2

Materials and Methods

Materials

The W_w dipeptides were purchased from DgPeptides (Hangzhou, China), iodine, deuterium oxide, sodium deuterioxide (NaOD) and deuterium chloride (DCl) were purchased from Sigma Aldrich (Rehovot, Israel). Water was processed by a Millipore purification system (Darmstadt, Germany) with a minimum resistivity of 18.2 M Ω cm.

Crystal preparation

The dipeptide powder was dissolved in water at a final concentration of 5.0 mg mL⁻¹. The solution was then incubated in an 80 °C water bath for 5 min, followed by filtration using 0.45 μ m PVDF membrane (Merck Millipore, Carrigtwohill, Ireland) and the pH was adjusted to 5.0-6.0 using NaOH and HCl. Needle-like colorless crystals appeared after a few minutes and reached maximum size after 30 days. Following centrifugation, the crystals were washed with water for three times and collected for further use.

Doping treatment

For iodine doping, the W_w crystals were sealed in a closed beaker with iodine powder for three hours. Upon the sublimation of iodine, the peptide sample was immersed in the iodine vapor and the color gradually changed from the original white into dark yellow. For neutrons doping, the dipeptide was crystallized in deuterium oxide rather than in normal water using the same procedure outlined above, and the solution pH was adjusted using NaOD and DCl.

Scanning electron microscopy (SEM)

The solution containing the crystals was placed onto a clean glass slide, allowed to adsorb for a few seconds and excess liquid was removed using a filter paper. The slide was then coated with Cr and observed under a JSM-6700 field emission scanning electron microscope (JEOL, Tokyo, Japan) operated at 10 kV.

X-ray crystallography

A dipeptide single crystal suitable for X-ray diffraction was coated with paratone oil (Hampton Research), mounted on a MiTeGen loop and flash frozen in liquid nitrogen. Diffraction data were recorded on a Bruker KappaApexII system with Mo K α radiation at 100 K. The data were processed with Apex2 Suite. The structure was determined by direct methods using SHELXT-2013 and refined by full-matrix least squares against F² with SHELXL-2013. The crystal data (cif. files) have been deposited in CSD with deposition numbers 1853728 and 1939621.

Computational band structures

Calculations were carried out using the Vienna *ab initio* simulation package VASP 5.3¹ within the framework of density functional theory. The projector augmented-wave (PAW) method was applied to treat both core and valence electrons.² The Kohn-Sham equations³ were solved using a plane-wave basis set, with an energy cut-off of 600 eV. To confirm the accuracy of computation, calculations using the range-separated hybrid Heyd-Scuseria-Ernzerhof (HSE)⁴ functional, with a range-separation μ of 0.11 bohr⁻¹ (HSE06),⁵ were carried out. All atomic geometries were fully relaxed until forces were less than 0.01 eV \AA^{-1} . $2 \times 2 \times 2$ k-point sampling was used for the monoclinic cell and a Gaussian smearing width of 0.05 eV was used for k space integrals.

UV-vis absorbance

The dried crystal samples were placed in a 96-well UV-Star UV transparent plate (Greiner BioOne, Frickenhausen, Germany). UV-vis absorbance was then recorded using a Biotek Synergy HT plate reader (Biotek, Winooski, VT, USA), with a normal reading speed and calibration before reading.

Mass spectroscopy (MS)

The MS experiment was performed using a LCMS Xevo-TQD system including an Acquity model UPLC and a triple quad mass spectrometer (Waters, Massachusetts, USA). The positive electrostatic ionization (ES-) channel was used for analysis.

Fluorescent microscopy characterization

The crystal samples were casted onto clean glass slides, and the fluorescent microscopy measurements were performed using a Nikon Eclipse Ti Inverted Microscope (Nikon Instruments, Tokyo, Japan) under different filters at ambient temperature.

Fluorescence spectroscopy

For fluorescent emission characterizations, the crystal samples were dropped onto clean quartz slides, and the spectra were collected using a FluoroMax-4 Spectrofluorometer (Horiba Jobin Yvon, Kyoto, Japan) at ambient temperature. The excitation wavelength was set at 300-500 nm with a slit of 5 nm and a step of 5 nm, and the emission wavelength was set at 350-600 nm with a slit of 5 nm and a step of 2 nm. The blank quartz slide was used as background and subtracted. The maximal emission spectra were extracted and plotted. At least three measurements were performed and averaged for accuracy.

Proton conductivity

Alternating current impedance measurements were carried out using a Solartron SI 1260 impedance/gain-phase analyzer over a frequency range of 0.1 Hz to 10 MHz with an applied voltage of 10 mV. The relative humidity was controlled by a STIK Corp. CIHI-150B incubator. The sample was pressed to form a cylindrical pellet of crystalline powder (~2 mm thick × 5 mm in diameter) coated with carbon-pressed electrodes. Two silver electrodes were attached to either side of the pellet to form four end terminals (quasi-four-probe method). The proton conductivity activation energy was calculated using the Arrhenius equation (1),

$$\ln(\sigma) = \ln(A) - \frac{E_a}{R} \left(\frac{1}{T}\right) \quad (1)$$

Where σ is the proton conductivity in S cm⁻¹, A is the pre-exponential constant, E_a is the proton conductivity activation energy in J mol⁻¹, R is the gas constant (8.314 J mol⁻¹ K⁻¹), and T is the absolute temperature in K.

Young's modulus measurement

Atomic force microscopy (AFM) experiments were carried out using a commercial AFM (JPK, Nanowizard II, Berlin, Germany). The force curves were obtained using the commercial software from JPK and analyzed by a custom-written procedure based on Igor pro 6.12 (Wavemetrics Inc.). Silica cantilevers (SSS-SeIHR-50 Nanosensor Company) with a half-open pyramidal face angle of $\theta < 10^\circ$, tip radius: 2-10 nm, frequency in air: 96~175 kHz were used in all experiments. The spring constant of the cantilevers was in the range of 10~130 N m⁻¹. The

maximum loading force was set at 150 nN. All AFM experiments were carried out at room temperature. In a typical experiment, the W_w crystals were cast on the surface of the glass substrate and the cantilever was moved over the crystal at a constant speed of $15 \mu\text{m s}^{-1}$ guided by an optical microscope. The cantilever was held on the crystal surface at a constant force of 150 nN. Then, the cantilever was retracted and moved to another spot for the next cycle. The indentation fit was performed using an Igor custom-written program and manually checked after the fitting was complete. The curves were then fitted manually. Each approaching force-deformation curve was fitted in the range of 10 nm from the contact point, or from the maximum indentation depth to the contact point if the former was less than 10 nm. By fitting the approaching curve to the Hertz model (2), we could obtain the Young's modulus of the W_w crystals. Typically, 5-8 such regions ($10 \times 10 \mu\text{m}$, 600 pixels) were randomly selected on each crystal to construct the elasticity histogram.

$$F(h) = \frac{2}{\pi} \tan \alpha \frac{E_{GW}}{1 - \nu_{GW}^2} h^2 \quad (2)$$

where F is the stress of the cantilever, h is the depth of the W_w crystal pressed by the cantilever tip, α is the half angle of the tip, E is the Young's modulus of the crystal and ν is the Poisson ratio. We chose $\nu = 0.3$ in our calculations.

Point stiffness calculation

The measured point stiffness (k_{meas}) is comprised of the stiffness constants of the cantilever (k_{can}) and the crystals (k_{cry}). Assuming that the W_w crystal and the cantilever act as two springs oriented in a series, the point stiffness of the W_w crystal could be calculated using the following relation: Using equation (3) below and an averaged measured value for k_{meas} , the average stiffness of the W_w crystal could be calculated. To estimate the material property of the crystals, it was assumed that the mechanical behavior of the W_w crystal could be described as linear elastic, which is a good approximation for solids under small strains.

$$k_{cry} = \frac{k_{can} \cdot k_{meas}}{k_{can} - k_{meas}} \quad (3)$$

Piezoelectric force microscopy (PFM)

For PFM experiments, 3 single crystals from each sample were selected, and three sites along each crystal were chosen. At each of these 3 sites, 5 measurements were performed in a $2 \mu\text{m}^2$ area. This resulted in a maximum of 45 measurements for each material. PVDF ($d_{33} = 20.7 \text{ pm V}^{-1}$) was used as a positive control before the measurements. The d_{33} piezoelectric coefficient was calculated using equation (4):

$$d_{33}^{eff} \left(\frac{\text{pm}}{\text{V}} \right) = \frac{\text{Slope of piezoresponse curve} \left(\frac{\text{nA}}{\text{V}} \right)}{\text{Gain} \times \text{Input} \times \text{IOS} \left(\frac{\text{nA}}{\text{nm}} \right)} \times 1000 \quad (4)$$

Where the slope of piezo-response curve is the slope of the linear relationship between the piezo-response as measured by the photodiode system and the applied voltage; the IOS coefficient depends on the alignment of the laser on the tip and the reflectivity of the back surface of the tip, and is calculated from the slope of a force-distance curve performed on a hard substrate. The

gain and input are both experimental factors selected during scanning and in this case were both equal to 10.

To ensure the electrostatic effects of both the substrate and the system did not influence the measurements, a number of voltage sweeps were performed on negative control samples, namely copper, Kapton and glass. This allowed to test hard, soft, insulating and conductive non-piezoelectric samples for a response using the same setup and parameters as those used for measurements on peptides crystals. A noisy, nonlinear relationship was observed in all cases, with a considerably lower magnitude compared to the piezo-response of piezoelectric samples.

Fabrication of peptide-based power generator

Two 1.2×1.2 cm² silicon substrates were sputtered with silver film. Ww crystal powders were tightly sandwiched to form a film between two substrates and closely sealed by Kapton tape and polydimethylsiloxane (PDMS, sylgard 184) that served as a container for the peptide sample and as a spacer for the device. In order to prevent cracking of the substrate due to the impact force from the linear motor, the top substrate was drop-coated with a PDMS damping layer. Two copper wires were connected to the silver electrodes using carbon ink (JELCON CH-8 MOD2) to complete the device fabrication.

Characterization of the power generator.

The peptide-based power generator was vertically fixed onto a stainless-steel plate, which was mounted on a precision linear slide stage. A linear motor (E1100-RS-HC type with Force Control, LinMot) was used to periodically press the power generator. The outputs of the generator were recorded using a low noise voltage preamplifier (Stanford SR560), and a constant measurement drift was removed from the open circuit voltage data. The force was measured using a force sensor (DYZ-101, Bengbu Ocean Sensing System Engineering Co. Ltd). The generator and the measuring instruments were placed in a Faraday cage to avoid interference from the environment.

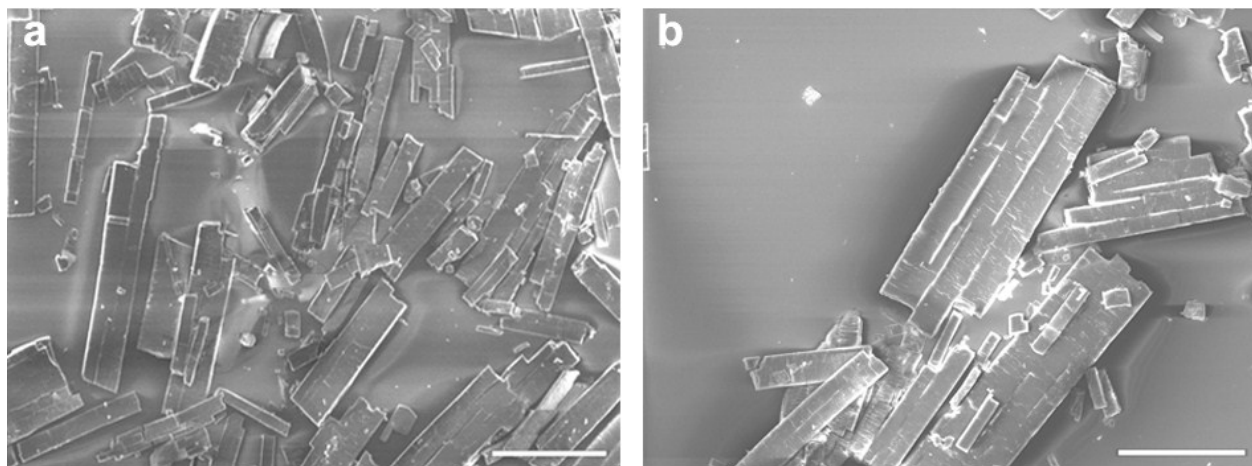


Fig. S1 SEM images of doped Ww crystals. a, Iodine-doped crystals. **b,** Neutron-doped crystals. Scale bar: 50 μm . As shown, the doping did not change the morphology of Ww assemblies (compare to Fig. 1a in the main text).

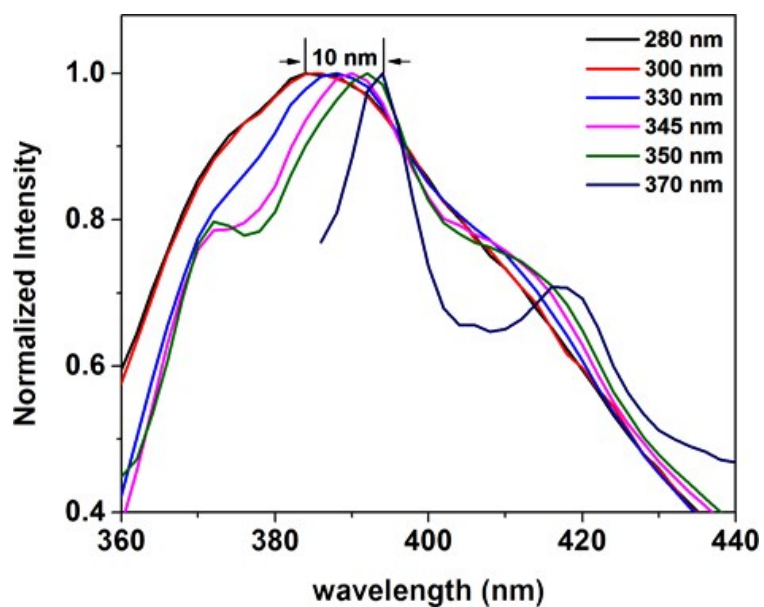


Fig. S2 Fluorescence emission of Ww crystals under different excitations. As the excitation wavelength red shifted, the maximal emission also red shifted by 10 nm, from 384 nm to 394 nm.

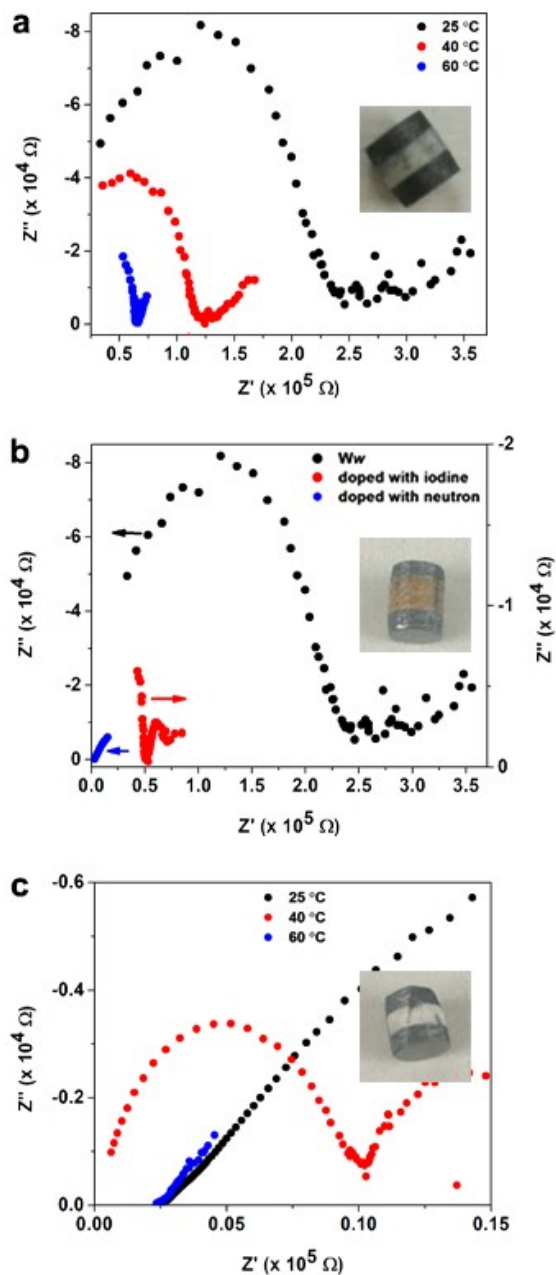


Fig. S3 Nyquist plot of the pristine and doped W_w crystals at 98% RH. a, Comparison of pristine W_w crystals at different temperatures. **b,** Comparison of pristine and doped W_w crystals at 25 °C. **c,** Comparison of W_w crystals prepared in deuterium oxide at different temperatures. The proton conductivity was calculated and is summarized in Fig. 3f in the main text. The insets show photographic images of the samples prepared for proton conductivity measurements.

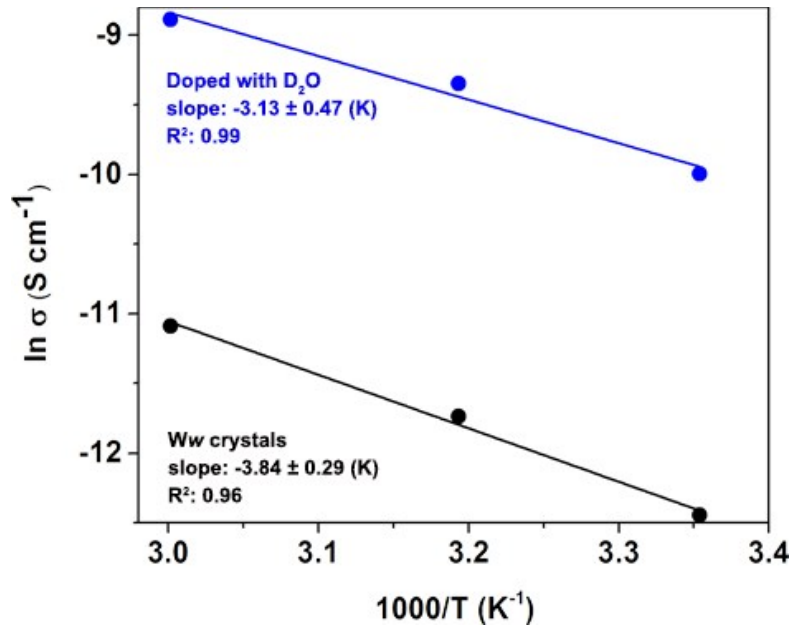


Fig. S4 Arrhenius-type plot of the conductivity (σ) as a function of the temperature for pristine and doped Ww crystals at 98% RH. The proton conductivity activation energy (E_a)

was calculated using the Arrhenius equation ($\ln(\sigma) = \ln(A) - \frac{E_a}{R} \left(\frac{1}{T}\right)$). The lines represent linear fittings of the data. The obtained slopes thus indicate the results of $-E_a/R$, and then E_a can be calculated.

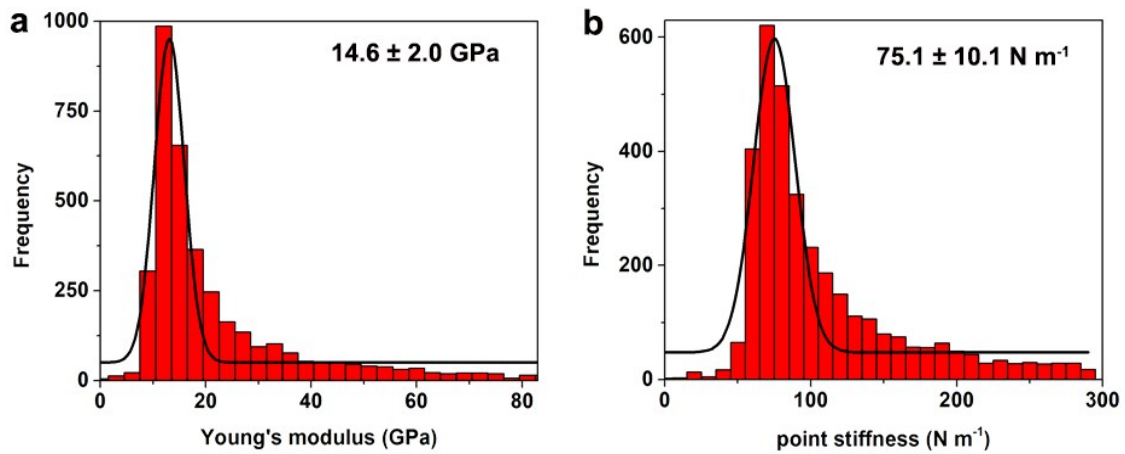


Fig. S5 Mechanical properties of the pristine Ww crystals. a, Young's modulus. **b,** Point stiffness. The normal distribution curves are also shown (black). At least 3500 counts were performed for statistics.

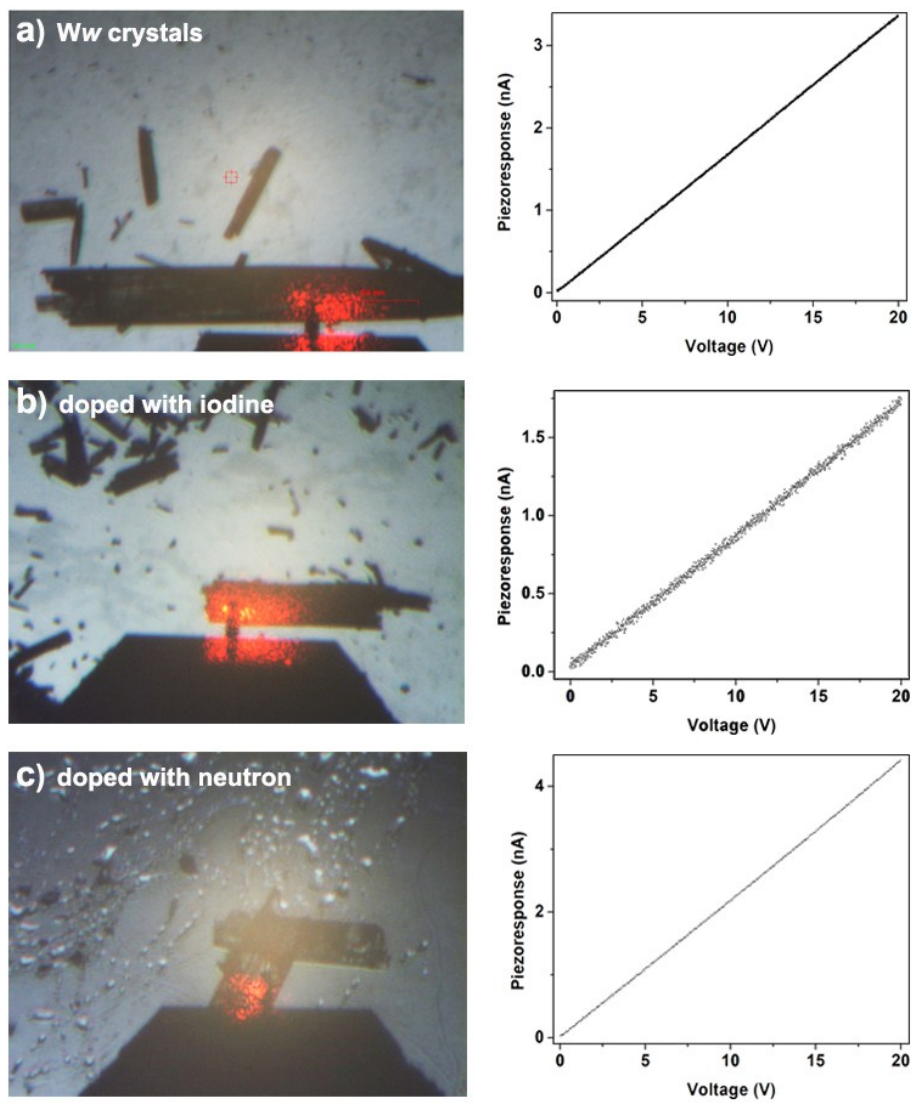


Fig. S6 Representative piezoelectric coefficient measurements using PFM. a, Pristine Ww crystals. **b,** Iodine-doped crystals. **c,** Neutron-doped crystals. In every row, the left panel shows a microscopy image of the sample during characterization and the right panel shows the linear relationship between the piezo-response as measured by the photodiode system versus the applied voltage.

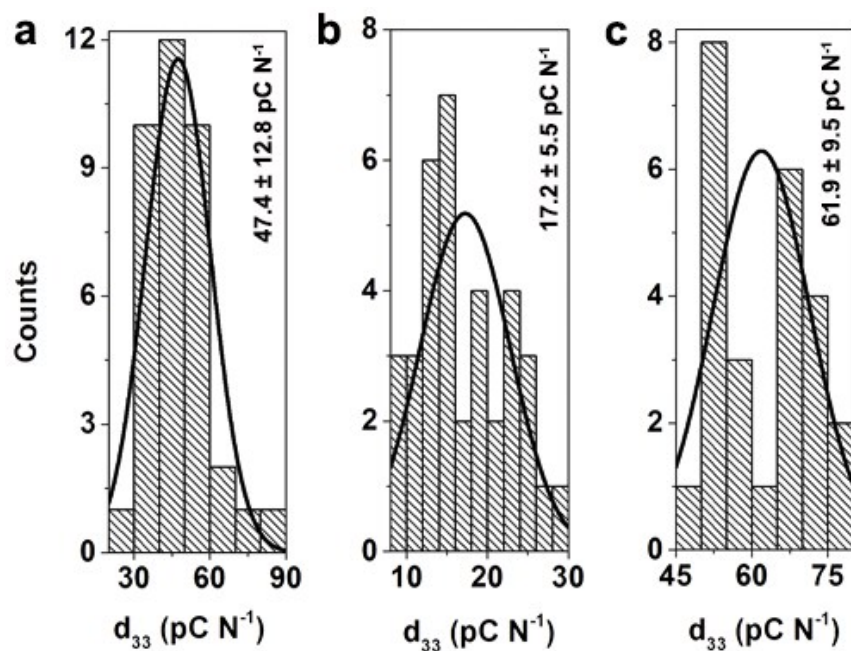


Fig. S7 Statistical distribution of the d_{33} coefficients of W_w crystals measured using PFM. **a**, Pristine W_w crystals. **b**, Iodine-doped crystals. **c**, Neutron-doped crystals.

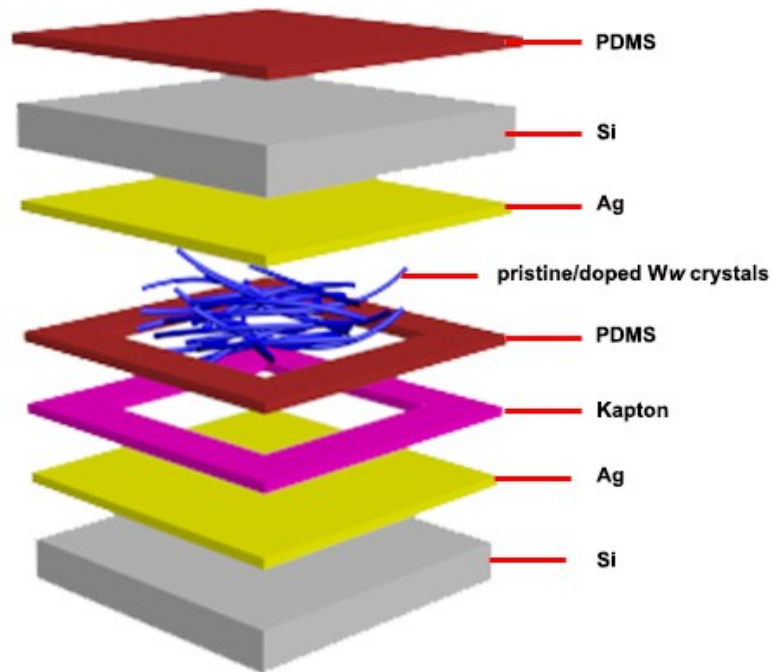


Fig. S8 Schematic drawing of the proof-of-concept generator fabricated using peptide crystals as the active components.

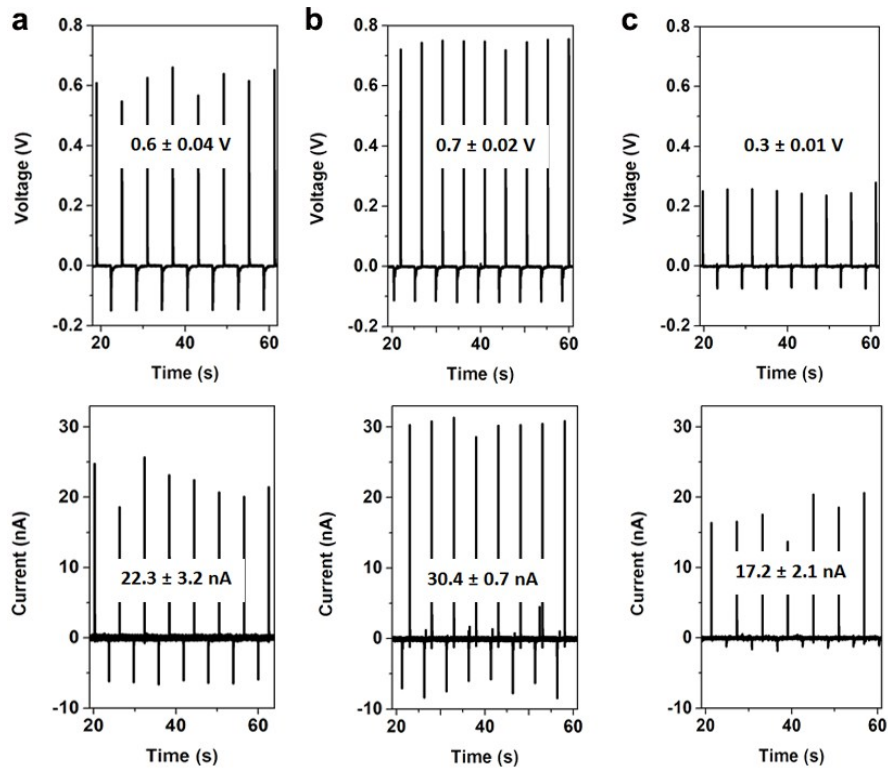


Fig. S9 Output signals from the generators utilized as a direct power source using Ww crystals as the active components. **a**, Pristine Ww crystals. **b**, Doped with neutrons. **c**, Doped with iodine. The pressing force was 38 N. In each column, the upper and lower panels show the open-circuit voltage and short-circuit current, respectively.

Cif S1. (separate file)

W_w crystal structure in normal water, CCDC Deposition Number 1853728.

Cif S2. (separate file)

W_w crystal structure in heavy water, CCDC Deposition Number 1939621.

References

- 1 G. Kresse and J. Furthmüller, *Comput. Mater. Sci.*, 1996, **6**, 15.
- 2 G. Kresse and D. Joubert, *Phys. Rev. B*, 1999, **59**, 1758.
- 3 W. Kohn and L. J. Sham, *Phys. Rev.*, 1965, **140**, A1133.
- 4 J. Heyd, G. E. Scuseria and M. Ernzerhof, *J. Chem. Phys.*, 2003, **118**, 8207.
- 5 A. V. Krukau, O. A. Vydrov, A. F. Izmaylov and G. E. Scuseria, *J. Chem. Phys.*, 2006, **125**, 224106.